Proposal Design: Mach-Zehnder Interferometer

Jirayu Mongkolkiattichai
National Astronomical Research Institute of Thailand (Public Organization)
260, Moo 4, Don Kaew Subdistrict, Mae Rim District, Chiang Mai, 50180, Thailand

I. Introduction

Photonic Technology relies on the manipulation of light in waveguide structures, which consist of a high-refractive-index (core) surrounded by a lower-refractive-index (cladding) medium. The properties of a waveguide can be engineered in proper ways, for example, with respect to dispersion, mode, and polarization. Many applications are realized using photonics, not only in telecommunication but also in sensing and quantum optics. A crucial tool in these applications is interferometry. Interferometers come in several forms, including the Michelson, Mach–Zehnder, and Fabry–Perot designs. In this discussion, I will focus on the Mach–Zehnder interferometer (MZI).

II. Theory

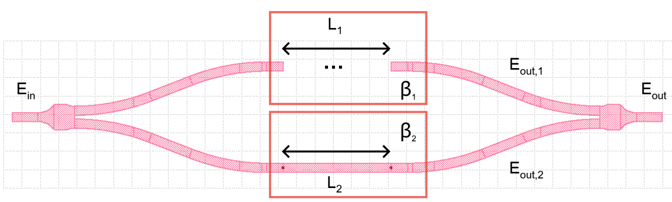

Fig. 1. **Schematic of a MZI. Light is split by a Y-branch and propagates along the upper and lower arms with different lengths. The light is then recombined by a Y-branch, resulting in a transmission profile.**

At the right end of the waveguides shown in Fig. 1, the electric field propagating along the upper and lower arms can be written as

$$E_{\text{out},i} = \frac{E_{\text{in}}}{\sqrt{2}} e^{-i\beta_i L_i - \frac{\alpha_i}{2} L_i}, \tag{1}$$

where E_{in} denotes the input field to the device, β_i represents the propagation constant and α_i is the propagation loss [1].

From the lecture, I learn that the output field from the last Y-brach is a combination of the fields from upper and lower arms, divided by the square root of two, i.e.,

$$E_{\text{out}} = \frac{1}{\sqrt{2}} \left(E_{\text{out},1} + E_{\text{out},2}\right). \tag{2}$$

The output field intensity is proportional to $|E|^2$, and I can express it as follows

$$I_{\text{out}} = \frac{I_{\text{in}}}{2} \left[1 + \cos(\beta_1 L_1 - \beta_2 L_2)\right], \tag{3}$$

where I treat $\alpha = 0$ as a special case in which propagation loss is absent. For an imbalanced interferometer with identical waveguides ($\beta_1 = \beta_2 = \beta$), I can simplify Eq. 3 to

$$I_{\text{out}} = \frac{I_{\text{in}}}{2} \left[1 + \cos(\beta \Delta L)\right]. \tag{4}$$

As can be seen, Eq. 4 is a sinusoidal function, and it is interesting to find the spacing between adjacent peaks, known as the free spectral range (FSR), which can be obtained by expressing

$$\text{FSR} = \Delta\lambda = \lambda_{m+1} - \lambda_m \tag{5}$$

where m is the spectral order. From the mode calculation, the effective index n is wavelength-dependent. As a result, the propagation constant is no longer constant across all wavelengths [2]. In fact, I can apply the first-order Taylor expansion of β such that

$$\beta_{m+1} \approx \beta_m + \frac{d\beta}{d\lambda}\Delta\lambda. \tag{6}$$

I rearrange this expression to get

$$\Delta\beta = \beta_m - \beta_{m+1} \approx -\frac{d\beta}{d\lambda}\Delta\lambda. \tag{7}$$

Let's consider $d\beta/d\lambda$, where $\beta = 2\pi n/\lambda$

$$\frac{d\beta}{d\lambda} = \frac{2\pi}{\lambda}\frac{dn}{d\lambda} + 2\pi n\left(-\lambda^{-2}\right) = -\frac{2\pi}{\lambda^2}\left(n - \frac{dn}{d\lambda}\lambda\right). \tag{8}$$

Finally, the FSR depends on three parameters: wavelength, path length difference, and the group index.

$$\text{FSR} = \Delta\lambda = \frac{\lambda^2}{\Delta L\left(n - \lambda\frac{dn}{d\lambda}\right)} = \frac{\lambda^2}{n_g \Delta L}. \tag{9}$$

III. Modeling and Simulation

Here, we consider a waveguide geometry with a height of 220 nm and a width of 500 nm, and TE polarization is assumed. The fundamental TE mode in the waveguide is calculated using Lumerical MODE as shown in Fig. 2. The software allows us to obtain several physical parameters

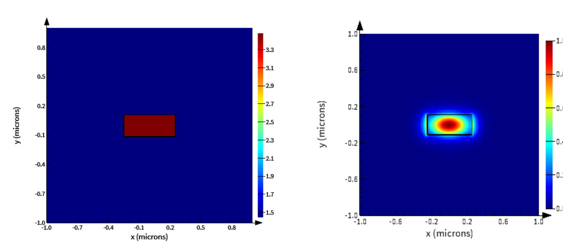

(a) (b)

Fig. 2. Fundamental Mode Simulation. (a) Waveguide schematic, (b) 2d intensity profile of the TE_{00} mode.

including effective index (n_{eff}), group index (n_g), loss, and effective area. It is interesting to study the variation of the effective index and the group index as a function of wavelength

(Fig. 3). The variation of n_{eff} is approximately 0.1, whereas n_g varies by about 0.01 for a wavelength range spanned by 100 nm centered at 1550 nm. The wavelength-dependent

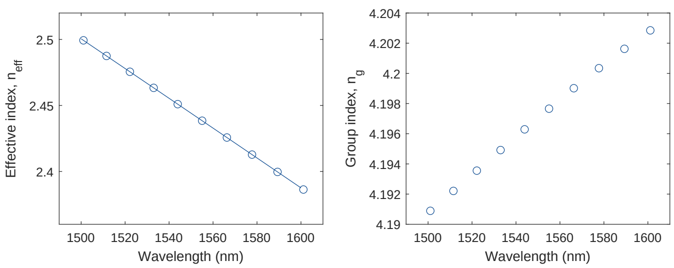

Fig. 3. **Effective and group indices.** (left) Effective index n_{eff} as a function of wavelength λ. The solid line indicates the compact model. (right) Group index n_g as a function of wavelength λ.

effective index can be understood using a compact model for the waveguide, which I express as a polynomial function. Here, I use a quadratic polynomial. By fitting the simulated data points in Fig. 3(a), I obtain $n_{\text{eff}}(\lambda)$ as follows:

$$n_{\text{eff}} = 2.4441 - 1.1290(\lambda - 1.55) - 0.0391(\lambda - 1.55)^2. \quad (10)$$

This dispersion of the indices governs the wavelength-dependent phase accumulation in the MZI which contains several components. To understand its behaviors, I analyze each component by calculating the transfer function. In practice, I input a constant optical power, sweep the wavelength, and measure the gain. This can be performed straightforwardly using Lumerical INTERCONNECT. As shown in Fig. 4, the Y-branch exhibits an approximately constant gain of about -3 dB, whereas the grating-grating coupler has a full width at half maximum (FWHM) of approximately 50 nm. The purpose of having two grating-grating couplers with different waveguide lengths is to measure a propagation loss (Fig. 4(d)).

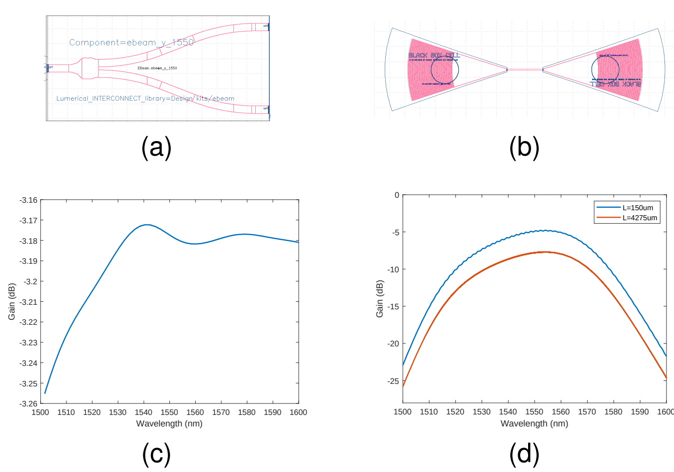

Fig. 4. **Transfer functions.** (a,c) Y-branch and its transfer function. (b,d) Grating–grating coupler and its transfer function for a short waveguide (150 μm) and a long waveguide (4275 μm).

By constructing the MZI from available components in the ebeam PDK, I prepared a system to run a full simulation (Fig. 5).

dL (μm)	calculated FSR (nm)	simulated FSR (nm)
50	11.4	11.2
100	5.7	5.6

TABLE I
MZI PARAMETERS.

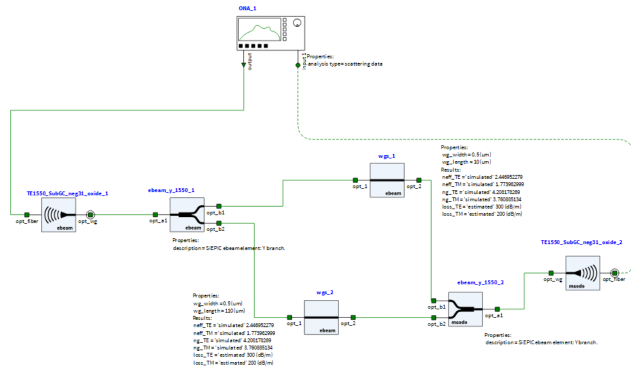

Fig. 5. **Schematic of MZI in Lumerical INTERCONNECT.**

I verify Eq. 9 by constructing Table I for the proposed MZIs. Both calculated FSR and simulated FSR are nearly identical, with only a slgight difference in the first decimal place. The simulation allows us to obtain the transfer function as demonstrated in Fig. 6. In the experiment, I will measure the transmission as a function of wavelength. I can extract the peak-to-peak spacing and determine the corresponding wavelength range which yields the FSR. The measured FSR is the subsituted into to Eq. 9, given the known path length difference between the MZI arms. The group index can then be directly obatined. The designed layout is illustrated in Fig. 7.

IV. Conclusion

I have proposed two MZIs that will be used to extract the group index from measurements. Variations in the group index reflect changes in the refractive index resulting from the deposition process during fabrication. In addition, the design includes a long waveguide, which can be utilized to calibrate the propagation loss. The remaining layout area is expected to accommodate additional devices prior to the hard deadline, including an arrayed waveguide grating (AWG).

References

[1] L. Chrostowski and M. Hochberg, *Silicon Photonics Design*. Cambridge, U.K.: Cambridge University Press, 2015.

[2] L. Chrostowski, "The free spectral range (FSR) of the imbalanced interferometer," presented at UBCx Phot1x course, EdX, Jan 2026.

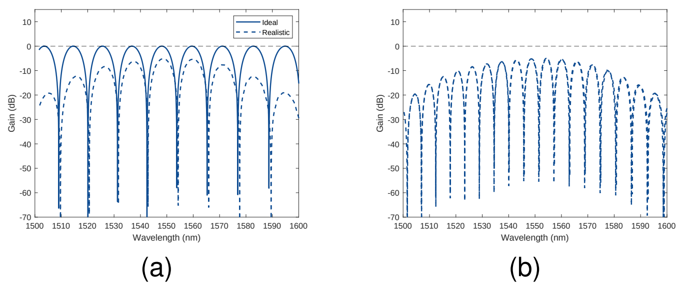

Fig. 6. **Transfer function of MZI.** (a) $dL = 50\mu m$ and (b) $dL = 100\mu m$. The solid line indicates an ideal case where no loss occurs and bandwidth is independent. The dashed line represents a realistic case that includes loss and wavelength dependence.

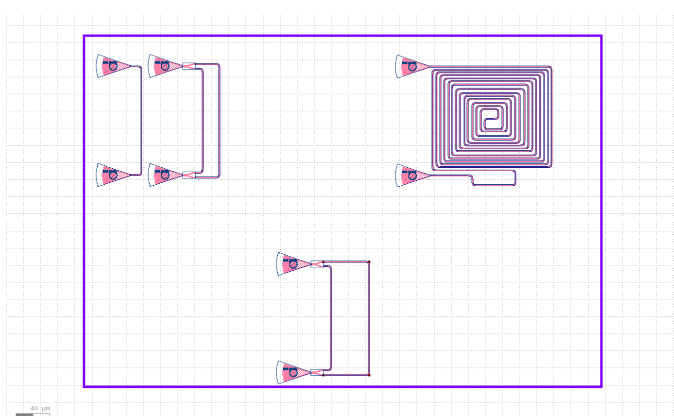

Fig. 7. **Layout of the designed MZI devices.**